

LARGE-AMPLITUDE X-RAY OUTBURSTS FROM GALACTIC NUCLEI: A SYSTEMATIC SURVEY USING *ROSAT* ARCHIVAL DATA

J. L. DONLEY,^{1,2} W. N. BRANDT,¹ MICHAEL ERACLEOUS,^{1,3} AND TH. BOLLER⁴

Received 2002 February 22; accepted 2002 June 12

ABSTRACT

In recent years, luminous X-ray outbursts with variability amplitudes as high as ≈ 400 have been serendipitously detected from a small number of active and inactive galaxies. These outbursts may result from the tidal disruptions of stars by supermassive black holes, as well as accretion disk instabilities. In order to place the first reliable constraints on the rate of such outbursts in the universe and to test the stellar tidal disruption hypothesis, we have performed a systematic and complete survey for them by cross-correlating *ROSAT* All-Sky Survey (RASS) and pointed Position Sensitive Proportional Counter data. We have detected five galaxies that were in outburst during the RASS, three of which show no signs of nuclear activity; these objects had been reported on individually in previous studies. After making reasonable corrections for the complicated selection effects, we conclude that the rate of large-amplitude X-ray outbursts from inactive galaxies in the local universe is $\approx 9.1 \times 10^{-6}$ galaxy⁻¹ yr⁻¹. This rate is consistent with the predicted rate of stellar tidal disruption events in such galaxies. When only the two active galaxies are considered, we find a rate for active galaxies of $\approx 8.5 \times 10^{-4}$ galaxy⁻¹ yr⁻¹. In order to place tighter constraints on these rates, additional outbursts must be detected.

Key words: galaxies: active — galaxies: nuclei — X-rays

1. INTRODUCTION

The detection of large-amplitude X-ray outbursts originating from inactive and active galactic nuclei (AGNs) has generated considerable interest. These outbursts have variability amplitudes up to a factor of ≈ 400 , decay over periods of months to years, often exceed outburst X-ray luminosities of 10^{43} – 10^{44} ergs s⁻¹, and usually have extremely soft X-ray spectra. Possible mechanisms considered to explain these events include (1) the tidal disruptions of stars by supermassive black holes, (2) accretion disk instabilities, and (3) the X-ray afterglows of gamma-ray bursts (e.g., Komossa & Bade 1999 and references therein). Many of the outbursts detected thus far are best explained by the stellar tidal disruption scenario. In addition, at least one of these outbursts appears to be consistent with the disruption of a brown dwarf or giant planet (Li, Narayan, & Menou 2002). A typical inactive galaxy is expected to undergo a tidal disruption event as often as every $\approx 10^5$ – 10^6 yr (e.g., Magorrian & Tremaine 1999, corrected for the lower black hole masses of Merritt & Ferrarese 2001 using the scalings relation of Frank & Rees 1976; D. Merritt 2002, private communication). The resulting emission from such an event should peak in the extreme ultraviolet or soft X-ray band, and it should decline over a period of roughly several months (e.g., Gurzadyan & Ozernoy 1980; Rees 1990). Of course, the observable effects of these events remain fairly uncertain because of the complexity of the disruption and subsequent accretion processes; an alternate spectral distribution in

which significant emission is radiated in the optical band has been investigated by Loeb & Ulmer (1997). Sembay & West (1993) predicted that at least several hundred and perhaps as many as several thousand tidal disruption events should have been detected during the *ROSAT* All-Sky Survey if a substantial fraction of galaxies contain supermassive black holes (SMBHs) of masses 10^7 – $10^8 M_{\odot}$; investigations of correlations between central black hole mass and bulge properties suggest that the latter is true (e.g., Ferrarese & Merritt 2000; Gebhardt et al. 2000). Detecting and understanding these events will aid in determining the importance of the stellar tidal disruption process in the fueling of SMBHs and may also lead to a better understanding of accretion disk instabilities (e.g., Siemiginowska, Czerny, & Kostyunin 1996; Burderi, King, & Szuszkiewicz 1998). X-ray outbursts could also be related to the creation of double-peaked emission lines in AGNs (e.g., Syer & Clarke 1992; Eracleous et al. 1995; Storchi-Bergmann et al. 1997) and nuclear outbursts seen at other wavelengths (e.g., Cappellari et al. 1999; Renzini et al. 1995).

The first large-amplitude X-ray outburst was detected in the galaxy E1615+061 using *HEAO 1* and *EXOSAT* (Piro et al. 1988).⁵ All subsequent X-ray detections have been made using data from *ROSAT*. *ROSAT* was especially sensitive in the soft (0.1–1.0 keV) band where the emission from these outbursts is expected to be strong, and it covered $\approx 20\%$ of the sky at least twice. Because constant monitoring of the X-ray sky or the comparison of at least two observations are the only ways to detect long-lived outbursts, *ROSAT* provided an excellent means by which large-amplitude X-ray outbursts could be found and investigated.

Of those galaxies caught undergoing X-ray outbursts, only E1615+061, IC 3599 (Brandt, Pounds, & Fink 1995;

¹ Department of Astronomy and Astrophysics, The Pennsylvania State University, 525 Davey Laboratory, University Park, PA 16802.

² NSF-supported undergraduate research associate.

³ Visiting Astronomer, Kitt Peak National Observatory and Cerro Tololo Inter-American Observatory, which are operated by the Association of Universities for Research in Astronomy, Inc., under a cooperative agreement with the NSF.

⁴ Max-Planck-Institut für extraterrestrische Physik, Postfach 1312, D-85741 Garching bei München, Germany.

⁵ We note, however, that a possible detection of a tidal disruption event was made in 1890 through the visual observation of the galaxy NGC 1068 (Packer 1891; de Vaucouleurs 1991).

Grupe et al. 1995a), and WPVS 007 (Grupe et al. 1995b) showed signs of nuclear activity prior to or after the outburst. E1615+061 is a Seyfert 1, IC 3599 is a Seyfert 1.9 (Komossa & Bade 1999), and WPVS 007 is a narrow-line Seyfert 1. NGC 5905 (Bade, Komossa, & Dahlem 1996), RX J1242.6–1119 (Komossa & Greiner 1999), RX J1420.4+5334 (Greiner et al. 2000), and RX J1624.9+7554 (Grupe, Thomas, & Leighly 1999) have optical spectra that show no signs of nuclear activity. Both NGC 5905 and RX J1624.9+7554 are spiral galaxies; the former is classified as an H II type. RX J1242.6–1119 is a pair of elliptical or early spiral galaxies likely to be interacting, and RX J1420.4+5334 is also an elliptical or early spiral galaxy. It is likely that these four galaxies harbor otherwise dormant SMBHs that became active in the X-ray band only following transient fueling events.

The X-ray outbursts detected thus far were found either (1) serendipitously through X-ray and optical follow-up observations of galaxies or unidentified objects with soft X-ray spectra and other interesting properties, or (2) serendipitously from *ROSAT* fields pointed at different targets. In order to place reliable constraints on the number of such outbursts that occur in the universe, more *systematic* and *complete* surveys must be performed. Here, we present the results of such a survey. By cross-correlating *ROSAT* All-Sky Survey (RASS) and pointed observations, we have identified all *ROSAT* sources at high Galactic latitudes that (1) were in outburst during the 6 month RASS and that (2) had count rates or upper limits a minimum factor of 20 lower in pointed observations taken before or after the RASS. We use the results of this survey to set the first reliable constraints on the frequency of large-amplitude X-ray outbursts in the universe. These constraints allow comparison with tidal disruption predictions such as those of Magorrian & Tremaine (1999), and they also allow assessment of the ability of *Chandra*, *XMM-Newton*, and future missions to identify additional outbursts of this type. We note that Komossa & Dahlem (2001) performed a similar survey for the nearby galaxies in the Ho, Filippenko, & Sargent (1995) sample and did not detect any additional large-amplitude X-ray outbursts. This work differs from ours in that X-ray outbursts were looked for only from previously known, nearby galaxies, whereas our survey looks for variability from all RASS sources.

Throughout this paper, values of $H_0 = 75 \text{ km s}^{-1} \text{ Mpc}^{-1}$ and $q_0 = 0.5$ have been assumed. Galactic column densities have been taken from either Heiles & Cleary (1979) or Stark et al. (1992) as appropriate.

2. THE SURVEY

2.1. Definition of the Survey

For the purpose of this survey, we define “large-amplitude X-ray outbursts” to be events in galaxies or quasars that cause their count rates to vary by a minimum factor of 20 in the 0.1–2.4 keV *ROSAT* energy band. A minimum variability factor of 20 was chosen because the X-ray emission of AGNs is known to vary by factors up to ≈ 10 –15 through the “normal” processes at work in them; we want to discriminate against “normal” AGN variability. In some extreme cases, moderately obscured AGNs (e.g., Seyfert 1.5, 1.8, and 1.9 galaxies) can vary by factors of ≥ 20 in the soft X-ray band because of changes in the amount of

absorption along the line of sight (e.g., the Seyfert 1.5 galaxy NGC 3516; see Guainazzi, Marshall, & Parmar 2001 and references therein). This behavior is not likely to be related to the X-ray outbursts that are the focus of this study, and below we shall discriminate against such objects to the greatest extent possible using optical classification information, X-ray spectral information, and the observed variability characteristics. While this introduces an element of subjectivity into our study, obscured objects with possible absorption changes are fortunately not a major source of confusion; only one such object was found in our survey, and it is discussed in more detail in § 3.1.2. For the purpose of excluding the most X-ray luminous young supernova remnants and X-ray binaries from our survey (e.g., Schlegel 1995; Makishima et al. 2000), we have also defined a minimum outburst X-ray luminosity threshold of $1 \times 10^{41} \text{ ergs s}^{-1}$.

In this survey, we focus solely on galaxies and quasars that were detected in outburst during the 6 month RASS and that were either detected or undetected in their low states in pointed *ROSAT* observations preceding or following the RASS. We have chosen to focus on this sample because the sensitivity of the typical pointed observation greatly exceeds that of the typical RASS observation. The pointed observations can therefore be used more effectively than the RASS observations to determine the low count rates and upper limits of these objects in quiescence.

We chose to search catalogs of the Position Sensitive Proportional Counter (PSPC) pointed data and not the data taken with the High Resolution Imager because the observations with the former cover $\approx 18\%$ of the sky, while those with the latter cover only $\approx 2\%$ of the sky. Our search of the cataloged PSPC observations was limited to radii $\leq 50'$ from the center of the PSPC field. The point-spread function of a source whose central position is located outside of this radius extends beyond the detector’s area, causing counts to be lost. For PSPC observations centered $\leq 3'$ apart, we searched only the field with the highest exposure time. While the addition of several PSPC fields is possible, the catalogs of pointed sources used in our cross-correlations do not use such added fields. Our sensitivity was therefore determined by the most sensitive observation in a given area of sky. The effect of this selection strategy is negligible, since most of the ≈ 700 overlapping fields removed have exposure times that are significantly lower than those of the longest exposures in each of these fields. Because of the high absorption column density and large number of confusing sources in the Galactic plane, we do not consider in our survey the region of the sky from Galactic latitudes of -30° to $+30^\circ$.⁶ All large-amplitude X-ray outbursts to date have been found outside this region of sky. We have also removed from our survey 138 PSPC fields whose 0.2–2.4 keV background count rates are greater than $1.4 \times 10^{-3} \text{ counts s}^{-1} \text{ arcmin}^{-2}$; these fields have reduced sensitivities because of their higher backgrounds, and their inclusion would introduce significant additional dispersion into the detection thresholds. With all of the above restrictions taken into account, our survey has searched $N_p = 1617$ pointed PSPC fields to radii of $50'$, a sky coverage of $\approx 9\%$. The mean and median exposure times of the fields searched are 8373 and 5995 s, respectively. These should be compared with a typical RASS exposure time of ≈ 500 s.

⁶ For completeness, however, we have searched for flaring objects in the Galactic Plane and we summarize our findings in the Appendix.

We have compared observations taken during the 6 month RASS (in 1990–1991) with both the small number of pointed PSPC observations taken during the months preceding the RASS and the large number of pointed PSPC observations taken during the ≈ 4 yr following the RASS, thus probing timescales ranging from months to years. Assuming that large-amplitude X-ray outbursts decline over periods of months to years, nearly all bright outbursts that occurred from the ≈ 6 months preceding the RASS to the end of the ≈ 6 month period of the RASS should be identifiable as outbursts if pointed data at their positions are available.

2.2. Methods and Analysis

2.2.1. X-Ray Cross-Correlations

To detect large-amplitude X-ray outbursts, we have cross-correlated the RASS Bright Source Catalogue (RASS-BSC; Voges et al. 1999) with both the 2nd *ROSAT* Source Catalog of Pointed Observations with the PSPC (ROSPSPCCAT)⁷ and the WGA Catalog of *ROSAT* Point Sources (WGACAT; e.g., Angelini et al. 2000).

We began by searching for objects that were detected in both the RASS and pointed observations. For each RASS source, we first determined whether the source was located within the inner 50' of a pointed PSPC observation. If a pointed observation at the source location was available, the source's offset from the center of the field was measured, and an appropriate search radius was determined. The positional error of *ROSAT* PSPC sources increases as the off-axis angle increases. We used a search radius that varied linearly from 40'' on-axis to 80'' at an off-axis angle of 50' (Micela et al. 1996; Boese 2000, 2002; M. Corcoran & S. Snowden 2002, private communication).⁸ For each RASS source, we then searched both the ROSPSPCCAT and WGACAT catalogs for sources within the appropriate search radius of the RASS position whose count rates differed from the RASS count rate by a minimum factor of 10. Although our survey itself is constrained to sources with factors of variability of 20 or greater, we manually examined all sources with factors of variability above 10, so as not to miss sources variable by a factor ≥ 20 whose catalog count rates were slightly incorrect. Both the RASS and pointed vignetting-corrected count rates were calculated directly from the data using the ASTERIX package (Allan & Vallance 1995) to ensure that all measurements were uniform. The individual analysis of all candidates was necessary to avoid problems such as the shadowing of sources by the entrance window supports, catalog errors, and source confusion.

We also searched for objects that were detected in the RASS and undetected in pointed observations. Specifically, we looked for RASS sources for which a pointed PSPC observation at the source position was available but no counterpart was found within the appropriate error circle of the source position in either the ROSPSPCCAT or WGACAT catalogs. Due to sources missed by the pointed catalogs, positioning errors, and shadowing of sources by the entrance window supports, only a small percentage of the objects returned by this search were actually highly variable.

In order to determine which objects were valid candidates, pointed PSPC images of all of the sources returned by our search were examined. If a bright PSPC source from a pointed observation was clearly present at the RASS source position, we removed the source from the list of candidates. If a dim source was present, the count rates were calculated to search for variability by a factor of ≥ 20 . The distinction between undetected sources and sources with low count rates was made using the source searching program PSS (Allan 1995) in the ASTERIX package. To determine the upper limits on undetected sources, the 95% encircled energy radius of the point-spread function was calculated. A 3σ upper limit was set by dividing the square root of the number of counts within this radius by 0.95 and then multiplying this number by three. This method, which is used throughout the paper, gives upper limits that are generally consistent with those calculated using PSS in upper limit mode.

3. RESULTS

3.1. Sources Found in the Survey

3.1.1. Outbursts Detected

Our survey has recovered all of the previously known large-amplitude X-ray outbursts that were in a high state during the RASS and has detected one interesting X-ray variable galaxy, SBS 1620+545. The properties of the large-amplitude X-ray outbursts detected in our survey can be found in Table 1. In addition to large-amplitude X-ray outbursts from galaxies and AGNs, four previously known cataclysmic variables were detected in our survey (1E 1339.8+2837, RE J2316–05, UW Pic, and EV UMa). We used SIMBAD to identify these variable sources. We have therefore identified all X-ray sources with variability amplitudes ≥ 20 in our survey sample.

The observed variability amplitudes of the extragalactic outbursts range from ≈ 21 (RX J1420.4+5334) to ≈ 392 (WPVS 007). The observed variability amplitudes are lower limits to the true variability amplitudes, since it is possible that the outbursts were not caught at maximum in the RASS or were not at their lowest flux in earlier or later pointed observations.

The peak observed 0.2–2.4 keV luminosities of the detected outbursts range from $\approx 5 \times 10^{41}$ to $\approx 6 \times 10^{43}$ ergs s^{-1} . These values have significant uncertainties because of the steepness of the outburst spectra, all of which are moderately or extremely soft (see § 3.2 for further discussion). The spectra of WPVS 007 and NGC 5905 are especially soft, with hardness ratios (HR1; see Table 1) of -0.92 and -0.87 , respectively, placing them among the softest galaxies detected in the RASS. Because the spectra of most of the outbursts are very soft, their detection is greatly limited by high Galactic column densities. In our survey, the maximum Galactic column density through which a large-amplitude X-ray outburst was detected is 3.8×10^{20} cm^{-2} . The median Galactic column density toward these sources is 1.4×10^{20} cm^{-2} .

Several of the sources detected show variability *during* the RASS. The count rate of NGC 5905 increases by a factor of ≈ 3 in 4 days (Bade et al. 1996). Likewise, WPVS 007 shows an increase in count rate by a factor of ≈ 2 in 2 days (Grupe et al. 1995b). The RASS count rate of RX J1624.9+7554 is

⁷ See <http://wave.xray.mpe.mpg.de/rosat/rra/rospsc>.

⁸ See also Figures 1a and 1b of the unpublished report by Haberl et al. at ftp://ftp.xray.mpe.mpg.de/rosat/catalogues/lrxp/wga_rosatsrc.html.

TABLE 1
LARGE-AMPLITUDE X-RAY OUTBURSTS IN THE SURVEY

Name	α (J2000.0)	δ (J2000.0)	N_H^a	z	Amp _{var} ^b	Phase	Date	CR ^c	HR1 ^d	Γ^e	F_X^f	L_X^g	f^h	Ref.
WPVS 007.....	00 39 15.8	-51 17 03	2.6	0.0288	392	RASS	1990 Nov 10-12	1.02 ± 0.07	-0.92 ^{+0.09} _{-0.10}	8.3	5.66 ± 0.53	0.859	0.17	1
IC 3599.....	12 37 41.2	+26 42 27	1.3	0.0215	225	Pointed	1993 Nov 11-13	0.0026 ± 0.0013	-0.59 ^{+0.27} _{-0.31}	4.2	0.028 ± 0.012	0.0019
RX J1420.4+5334.....	14 20 24.4	+53 34 12	1.2	0.147	>21	RASS	1990 Dec 10-11	5.18 ± 0.11	-0.52 ^{+0.02} _{-0.07}	3.1	32.33 ± 0.76	2.77	0.40	2,3
NGC 5905.....	15 15 23.2	+55 31 05	1.4	0.0126	45	Pointed	1993 Jun 17	0.023 ± 0.004	-0.87 ^{+0.07} _{-0.19}	4.1	0.093 ± 0.018	0.0080
RX J1624.9+7554.....	16 24 56.5	+75 54 56	3.8	0.0636	>42	RASS	1990 Dec 5-8	0.31 ± 0.02	-0.88 ^{+0.09} _{-0.10}	5.8 ± 0.6	0.95 ± 0.09	3.21	0.03	4
						Pointed	1990 Jul 19-23	≤0.016
						RASS	1990 Jul 11-16	0.33 ± 0.02	-0.87 ^{+0.07} _{-0.08}	4.0 ± 0.4	1.71 ± 0.11	0.0509	0.06	5
						Pointed	1993 Jul 18	0.0073 ± 0.0011	-0.11 ^{+0.14} _{-0.14}	2.4 ± 0.7	0.045 ± 0.009	0.0014
						RASS	1990 Oct 7-15	0.54 ± 0.02	-0.08 ^{+0.04} _{-0.04}	3.3 ± 0.2	8.85 ± 0.43	6.24	0.23	6
						Pointed	1992 Jan 13	≤0.013

NOTE.—Units of right ascension are hours, minutes, and seconds, and units of declination are degrees, arcminutes, and arcseconds.

^a Galactic column density in units of 10^{20} cm⁻².

^b Observed amplitude of count-rate variability in the 0.1–2.4 keV band.

^c Count rate in the 0.1–2.4 keV energy band in counts s⁻¹.

^d HR1 = $(H - S)/(H + S)$, where S is the 0.1–0.4 keV count rate and H is the 0.4–2.4 keV count rate.

^e The photon indices of the outbursting galaxies were taken from the respective papers cited and are the best fits for power-law models with the column density fixed at the Galactic value. For WPVS 007, the pointed-phase photon index was estimated from the hardness ratio.

^f Observed-frame absorption-corrected X-ray flux from 0.2–2.4 keV in units of 10^{-12} ergs cm⁻² s⁻¹. See § 3.2 for discussion.

^g Observed-frame absorption-corrected X-ray luminosity from 0.2–2.4 keV in units of 10^{43} ergs s⁻¹. See § 3.2 for discussion.

^h F is the correction factor applied to each outburst's differential number count. See § 3.2.3 for discussion.

REFERENCES.—(1) Grupe et al. 1995b; (2) Brandt et al. 1995; (3) Grupe et al. 1995a; (4) Greiner et al. 2000; (5) Bade et al. 1996; (6) Grupe et al. 1999.

TABLE 2
THE X-RAY VARIABLE GALAXY SBS 1620+545

Name	α (J2000.0)	δ (J2000.0)	N_H^a	z	Amp _{var} ^b	Phase	Date	CR ^c	HR1 ^d	Γ^e	F_X^f	L_X^g
SBS 1620+545.....	16 21 45.1	+54 27 24	1.9	0.0516	20	RASS	1991 Jan 14-22	0.15 ± 0.01	+0.69 ^{+0.123} _{-0.131}	0.96	2.185 ± 0.280	1.11
						Pointed	1993 Sep 22-24	0.0074 ± 0.0024	+0.31 ^{+0.032} _{-0.199}	...	0.085 ± 0.084	0.043

^a Galactic column density in units of 10^{20} cm⁻².

^b Observed amplitude of count-rate variability in the 0.1–2.4 keV band.

^c Count rate in the 0.1–2.4 keV energy band in counts s⁻¹.

^d HR1 = $(H - S)/(H + S)$, where S is the 0.1–0.4 keV count rate and H is the 0.4–2.4 keV count rate.

^e The photon index was estimated from the hardness ratio.

^f Observed-frame absorption-corrected X-ray flux from 0.2–2.4 keV in units of 10^{-12} ergs cm⁻² s⁻¹. See § 3.2 for discussion.

^g Observed-frame absorption-corrected X-ray luminosity from 0.2–2.4 keV in units of 10^{43} ergs s⁻¹. See § 3.2 for discussion.

observed to vary about the mean by a factor of ≈ 2 on the timescale of a day (Grupe et al. 1999).

3.1.2. SBS 1620+545

Our survey has identified X-ray variability by a factor of ≥ 20 from SBS 1620+545; to our knowledge, this variability has not been reported previously. This object has been classified as a Seyfert 2 galaxy ($z = 0.0516$) by Carrasco et al. (1998) and as a Seyfert 1.9 galaxy by Veron-Cetty & Veron (1998), but it has not been studied further until this survey. The properties of SBS 1620+545 can be found in Table 2. Figure 1 shows the RASS positional error circle overlaid on a digitized Palomar Observatory Sky Survey (POSS) image of the galaxy. It is clear that the variable RASS source is located in the galaxy SBS 1620+545. The spectral shape of the observed X-ray emission, however, differs from those of the large-amplitude X-ray outbursts detected thus far. In contrast to the low hardness ratios of the outbursts detected in our survey, the hardness ratio (HR1) of SBS 1620+545 during the RASS was 0.69. The hard spectrum of the observed emission, in combination with the optical classification and relatively low factor of variability, lead us to suspect that the variability of this object may not have been due to the same mechanism at work in the large-amplitude X-ray outbursts that are the focus of this study (see § 2.1 for

further discussion). Instead, it is likely that the variability is due to changing absorption along the line of sight. We note that, because the X-ray spectrum of SBS 1620+545 is softer when the count rate is lower, complex absorption changes (due to, perhaps, a partially covering or ionized absorber) would be needed to explain the observations. It is also possible that SBS 1620+545 underwent an intrinsic spectral change. We consequently exclude SBS 1620+545 from our $\log N$ - $\log S$ analyses below, although it is an interesting object needing further study.

3.2. Number Counts

We have constructed $\log N$ - $\log S$ plots of the large-amplitude X-ray outbursts detected in our survey. We consider the cases in which all outbursts from galaxies and AGNs are included, in which only inactive galaxies are included, and in which only active galaxies are included (see § 3.2.4). These plots can be found in Figure 2. Because of the steepness of the outburst spectra, the flux measurements in these plots are for the 0.2–2.4 keV range. If the 0.1–2.4 keV range had been used, a large fraction of the absorption-corrected flux would be that from 0.1–0.2 keV. Because absorption prevents us from detecting many photons from 0.1–0.2 keV (i.e., the spectrum from 0.1–0.2 keV has not been well measured), it can be dangerous to extrapolate a steep power

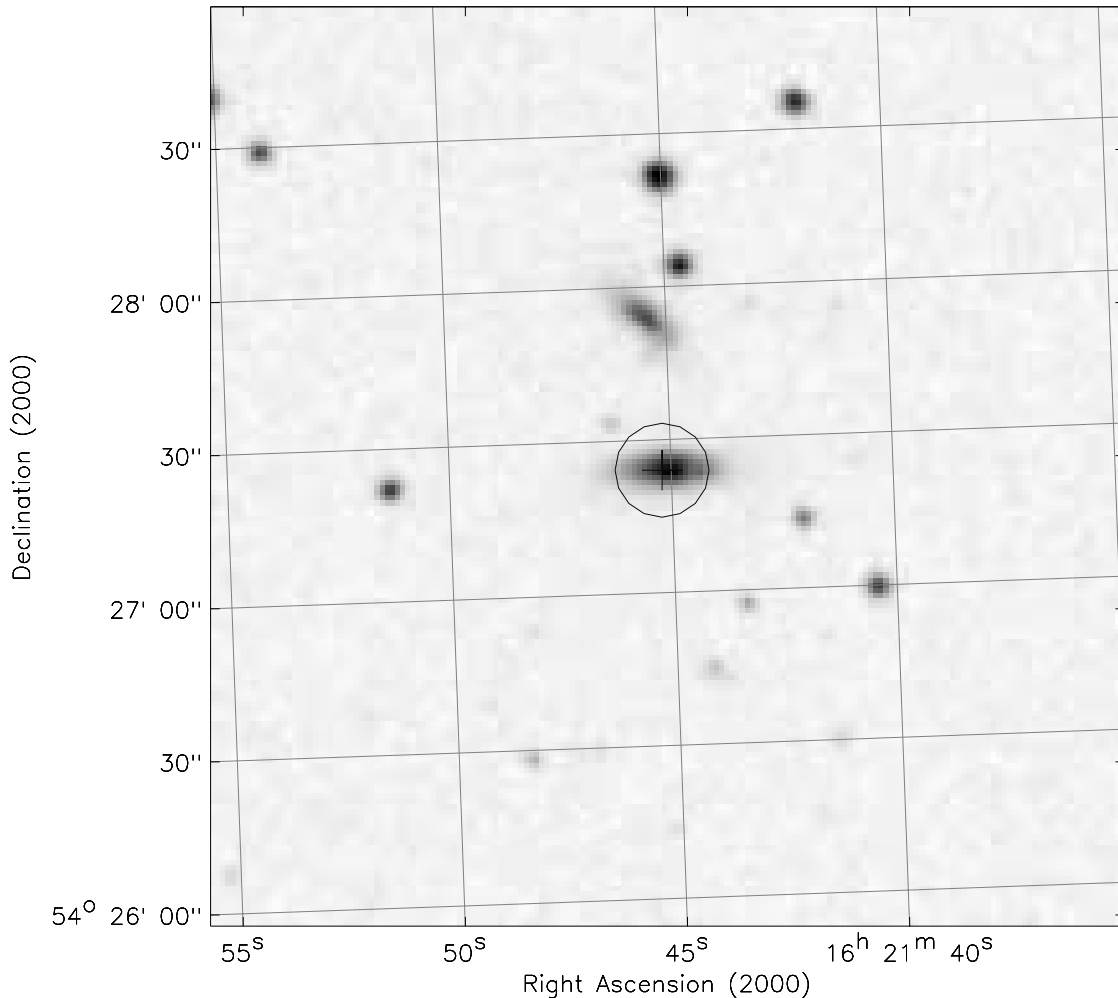


FIG. 1.—POSS image of the galaxy SBS 1620+545 with the $9''$ radius RASS positional error circle overlaid

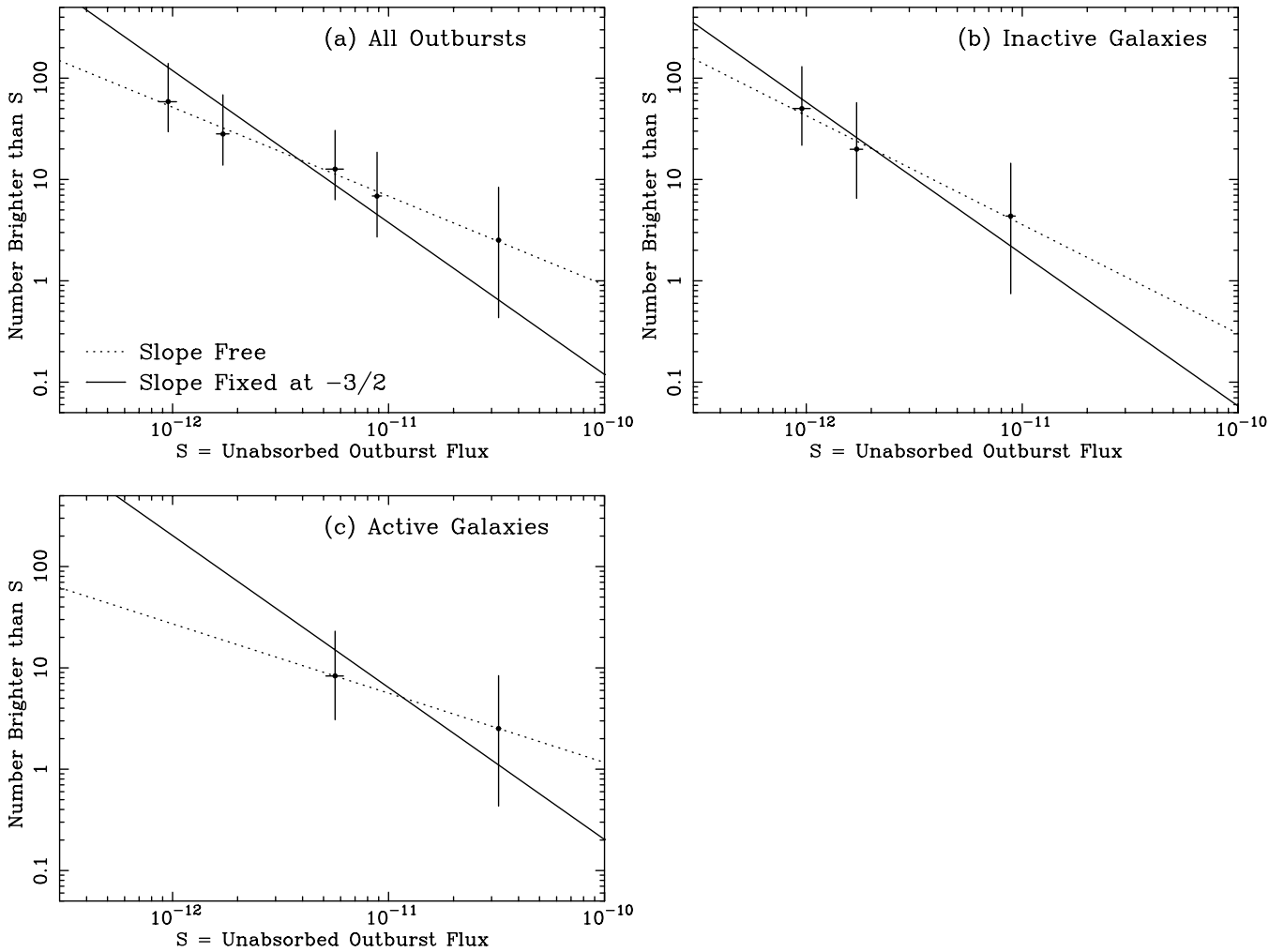


FIG. 2.—Corrected $\log N$ - $\log S$ plots for X-ray outbursts during the RASS. All outbursts from galaxies and AGNs are plotted in (a). In (b), only the inactive galaxies are plotted. The active galaxies are plotted in (c). We have separated the active and inactive galaxies because it is possible that a different mechanism is responsible for the large-amplitude X-ray outbursts arising from these two groups of objects.

law down to 0.1 keV (e.g., see § 2.3 of Brandt et al. 1999). Significant errors can also arise because of the poor constraints on the true spectral shapes of these outbursting objects. By removing the 0.1–0.2 keV range, we help to reduce the dependence of a source’s absorption-corrected flux upon its assumed low-energy spectral shape.

The number counts in Figure 2 have been corrected for the coverage of our survey, as discussed below in §§ 3.2.1–3.2.3; they consequently represent the number of outbursts expected to have occurred throughout the entire sky during the time period probed by our survey, assuming that intrinsic absorption does not prevent the detection of such outbursts. If intrinsic absorption is significant, our estimate of the true number of outbursts that occur in the universe will increase (see § 4.1 for further discussion).

3.2.1. Selection Effects

It was necessary to correct for two count-rate-dependent selection effects: (1) the existence of pointed PSPC data at the position of an outburst with a given count rate and (2) the probability that the exposure times of these observations are of sufficient length for the quiescent galaxy’s count rate

or upper limit to be measured to the accuracy needed to verify variability by a factor ≥ 20 . Our goal in correcting for these factors was to determine, as a function of absorption-corrected flux, the fraction of outbursts that were detected by our survey, thus allowing the observed number of outbursts at a given flux to be converted to the true number of outbursts at that flux. This correction was applied to the differential number counts.

Pointed PSPC data at a given outburst’s position can exist for one of two reasons; either (1) the outburst was followed up intentionally with the PSPC, or (2) it was observed serendipitously in a pointed PSPC field aimed at a different target. As we show below, X-ray bright galaxies are more likely to have been followed up intentionally with the PSPC than X-ray faint galaxies. In addition, the probability that the pointed count rate or upper limit of a galaxy caught serendipitously in a PSPC field can be measured to the accuracy needed to verify variability by a factor of ≥ 20 is higher for bright galaxies than for faint galaxies. Consequently, outbursts with high fluxes are more likely to have been discovered than outbursts with low fluxes. The fraction of the sky, F , in which outbursts with a given flux would have been

discovered was determined based on these selection effects. Here and hereafter, we consistently neglect the region of the sky from Galactic latitudes of -30° to $+30^\circ$ in our calculations (see § 2.1). To carry out the calculation of F , we assume that the outbursting galaxies are distributed isotropically, a valid assumption for extragalactic sources.

The fraction F is the sum of two components. The first, F_f , is the fraction of the sky in which a RASS source with a given flux would have been likely to be followed up intentionally with the PSPC, thus allowing the outburst to be discovered. The second, F_s , is the fraction of the sky in which a RASS source would not have been intentionally followed up, but the outburst would have been located serendipitously in a PSPC field aimed at a different target. We note that these corrections are intended to determine the flux-dependent fraction of the sky in which *any* large-amplitude X-ray outburst from a galaxy or AGN, not only the five that were found in our survey, would have been detected. Because the corrections are not being made for the specific outbursts detected, but rather to account for those outbursts from galaxies and AGNs that were *not* detected, the median photon index ($\Gamma = 4.0$) of the large-amplitude X-ray outbursts in our survey is used below in the calculation of the correction factor.

3.2.2. Probability of Intentional Follow-up

In order to estimate F_f , we first quantified the effect that an extragalactic source's RASS flux had on its probability of being followed up with the PSPC. To do so, we used Version 2.0 of the Hamburg/RASS Catalog of Optical Identifications (Bade et al. 1998). This catalog contains optical identifications for 4665 RASS-BSC sources in the extragalactic northern sky, and it was published after the PSPC ceased operation. Objects in this catalog were classified using the objective prism and direct plates taken by the Hamburg Quasar Survey (HQS). Although $\approx 20\%$ of the RASS-BSC sources in this catalog are listed as either "unidentified" or "empty," the majority of such sources are believed to be extragalactic; we therefore consider all "unidentified" and "empty" sources to be extragalactic. Consequently, the Hamburg/RASS catalog allowed us to identify all extragalactic RASS-BSC sources in the region of sky covered by the HQS. By cross-correlating the positions of the extragalactic Hamburg/RASS sources with the central positions of the pointed PSPC observations used in our survey, we were able to determine the percentage of extragalactic RASS-BSC sources with a given count rate that were intentionally followed up with pointed PSPC observations. This function, $P(R_o)$, where R_o is the observed RASS count rate, can be found in Figure 3. Because large-amplitude X-ray outbursts tend to be soft, we also measured $P(R_o)$ for only the extragalactic sources in the Hamburg/RASS catalog with negative hardness ratios (HR1). This function does not differ significantly from that for all extragalactic Hamburg/RASS sources.

To determine F_f , we considered $N_s = 92$ approximately equally spaced points on the high Galactic latitude survey sky. At each point, the Portable Interactive Multi-Mission Simulator (PIMMS; Mukai 2000) was used to calculate the expected RASS count rate, R_n , of an outburst with a given flux, based on the Galactic column density toward that position. The probability that an outburst with a given flux would have been followed up at one of these points is given

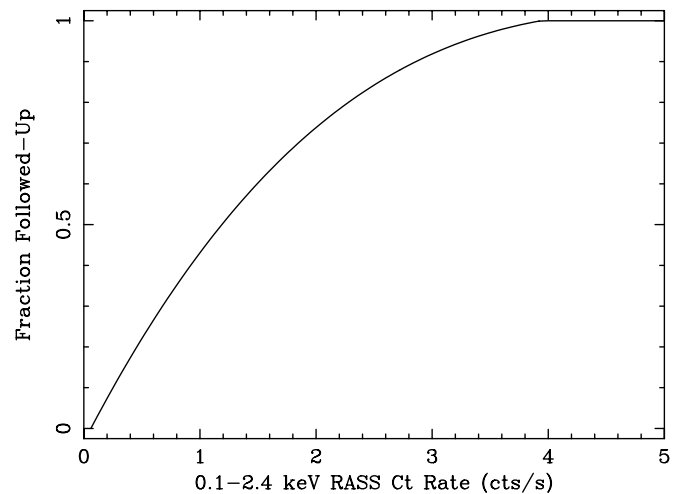


Fig. 3.—Fit to the fraction of extragalactic Hamburg/RASS sources that were followed up with pointed PSPC observations as a function of their RASS count rate.

by the value of the function $P(R_n)$ at this point, and it is taken to be equivalent to the probability that it would have been followed up if it were located in the area of the sky, $A = A_{\text{survey}}/92$ nearest this point, where $A_{\text{survey}} = 20,627 \text{ deg}^2$ is the area of the sky outside of the Galactic plane as defined in § 2.1. The fraction of the sky sampled by our survey in which the outburst would have been followed up and subsequently discovered is then given by

$$F_f = \sum_{n=1}^{N_s} \frac{P(R_n)}{N_s}. \quad (1)$$

3.2.3. Probability of Serendipitous Detection

To calculate F_s at each of the fluxes at which an outbursting galaxy was detected, we first found $A(R_l)$, the area of a given PSPC field in which a limiting on-axis count rate, R_l , would have been detected. To do so, a vignetting-corrected limiting count rate was calculated at 15 off-axis angle intervals of $3/33$. At each off-axis angle interval, we measured the number of background counts within the 95% encircled-energy radius of the appropriate point-spread function at that off-axis angle. The 3σ limiting count rate was then calculated as described in § 2.2.1. To normalize this function, we then divided the minimum detectable count rate, R_b , by the central minimum detectable count rate, R_C , converting $A(R_l)$ to $A(R_l/R_C)$ (the calculation of R_C is discussed below). We found this relationship for several PSPC observations covering a range of *ROSAT* exposure times. Although this function is slightly different for each PSPC observation, its overall shape and limits are largely consistent between the observations we have used here, once the background level is properly accounted for (recall also that PSPC fields with unusually high backgrounds were removed from the survey in § 2.1.) Because of this consistency, we were able to average the results of several PSPC observations to determine an average $\bar{A}(R_l/R_C)$ function. To create an observation-specific function $\bar{A}(R_l)$ for each PSPC field searched, we scaled the function $\bar{A}(R_l/R_C)$ by the central limiting count rate, R_C , of each observation. The equation for the central limiting count rate as a function of exposure time for

ROSAT PSPC observations was taken from § 10.1 of Appendix F of the *ROSAT* Mission Description. We made the assumption that a minimum of 10 counts is required to constitute a detection at the center of a PSPC field. The background count rate for each field was taken from either the ROSPSPCCAT or WGACAT catalogs; the appropriate corrections were made to convert the background count rates to the 0.2–2.4 keV energy band. The calculation of the central limiting count rate was performed for a signal-to-noise ratio of 3 and an enclosed source count fraction of 0.95.

To calculate the area of a given PSPC field in which the quiescent count rate or upper limit of an outbursting galaxy would have been measurable to the accuracy needed to demonstrate variability by a factor ≥ 20 , we measured the value of $\bar{A}(R_l)$ at $R_l = R_n/20$. Recall from § 3.2.2 that R_n is the expected RASS count rate at a given position for an outburst with a given flux, and therefore $R_n/20$ is the limiting count rate at that position above which large-amplitude variability cannot be demonstrated. The area of a given pointed PSPC field in which an outburst would have been discovered if and only if it were detected serendipitously is given by the area of that field in which the count rate $R_n/20$ would have been measurable, $\bar{A}(R_n/20)$, times the probability that the outburst would not have been intentionally followed up. The value, F_s , is then given by scaling this area to the area of the sky probed by the survey, A_{survey} , and summing over all $N_p = 1617$ PSPC fields used in our survey:

$$F_s = \sum_{n=1}^{N_p} \frac{\bar{A}(R_n/20)}{A_{\text{survey}}} [1 - P(R_n)]. \quad (2)$$

The total fraction of the survey sky in which a given large-amplitude X-ray outburst would have been detected, F , is thus given by:

$$F = F_f + F_s = \sum_{n=1}^{N_s} \frac{P(R_n)}{N_s} + \sum_{n=1}^{N_p} \frac{\bar{A}(R_n/20)}{A_{\text{survey}}} [1 - P(R_n)]. \quad (3)$$

Because the region of the sky from Galactic latitudes of -30° to $+30^\circ$ constitutes half of the area of the sky, the final fraction, F , was divided by 2 to scale the results to the entire sky. The value of F used to correct the differential number count of each outburst detected in our survey is given in Table 1. While we recognize that correction for these complicated systematic effects is challenging, we believe that the method described above provides the best practical correction.

3.2.4. $\log N$ – $\log S$ Plots

To construct the corrected $\log N$ – $\log S$ plots, we first divided each outburst's differential number count, 1, by the fraction of the survey area in which an outburst with that flux would have been discovered, F . We then converted from differential number counts, $N(S)$, to cumulative number counts, $N(>S)$. The error bars on the corrected number counts have been calculated using small-number statistics as outlined in Gehrels (1986), i.e., it was assigned to be the small-number statistical error on 1 divided by F . When converting from differential to cumulative number counts, these errors were added in quadrature. We note that the points in Figure 2 lie roughly on straight lines. The reason for this behavior is that the correction function, F , as a function of

TABLE 3
NUMBER COUNT FITS: $N(>S) = A(S/10^{-12})^\alpha$

Parameters	A^a	α^a	Outbursts (galaxy $^{-1}$ yr $^{-1}$)
All outbursts, α free	$51.7^{+97.9}_{-33.84}$	-0.88 ± 0.60	1.2×10^{-5}
All outbursts, α fixed.....	$118.9^{+119.4}_{-59.6}$	-1.50	1.8×10^{-5}
Inactive galaxies, α free	$42.7^{+111.8}_{-30.9}$	-1.08 ± 1.03	9.0×10^{-6}
Inactive galaxies, α fixed ...	$58.0^{+99.8}_{-36.7}$	-1.50	9.1×10^{-6}
Active galaxies, α free	$27.2^{+1269.8}_{-26.6}$	-0.68 ± 1.49	2.0×10^{-4}
Active galaxies, α fixed.....	$202.5^{+521.9}_{-145.9}$	-1.50	8.5×10^{-4}

^a With 90% confidence errors ($\Delta\chi^2 = 2.71$).

flux, is nearly linear in log-log space. The corrected $\log N$ value for each point is determined entirely by this correction function. As such, the error bars on the number counts should not be interpreted as standard statistical errors, but are instead representative of the uncertainty introduced by the correction itself (i.e., as the correction to the differential number counts increases, the error bars on the corrected number counts increase). We believe that this method provides the most reasonable estimation possible of the complicated errors associated with this work.

In Figure 2a, we plot number counts derived using all of the large-amplitude X-ray outbursts that occurred during the RASS. In Figure 2b, we plot only those outbursts that originated from inactive galaxies, for which the stellar tidal disruption outburst scenario is most likely to be applicable. In Figure 2c, we plot those outbursts from active galaxies, for which accretion disk instabilities may be responsible. We have determined for each of the above cases both the best-fit power laws [$N(>S) \propto S^\alpha$] to the data points, as well as the best-fit power laws for fixed power-law indices of $\alpha = -3/2$; a power-law index of $-3/2$ is expected for a sample of uniformly distributed sources in Euclidean space. The fit parameters can be found in Table 3.

The best-fit α values for the cases in which all outbursts are considered and in which only inactive galaxies are considered are approximately -1 . The flatness of this parameter may be due to small-number statistical fluctuations or to the superposition of more than one population. Because of the small number of detected sources and the likely heterogeneity of the sample, it is difficult to rule out any of the number count fits; we consequently consider all cases when placing constraints on the frequency of large-amplitude X-ray outbursts in the local universe.

3.3. Survey Volume

To determine the characteristic outburst flux limit and volume to which our survey is complete, we converted the function $\bar{A}(R_l/R_C)$, the area of a given PSPC field in which a limiting on-axis count rate would have been detected, to its differential form. The resultant function, $\bar{A}_{\text{diff}}(R_l/R_C)$, gives the area of a PSPC field with a given limiting on-axis count rate. After scaling this function to each PSPC observation, we summed it over all PSPC fields used in this survey. This summed function gives the area of our survey with a given limiting absorption-corrected count rate and has a peak at 0.031 counts s^{-1} . We adopt this peak value as the characteristic 0.2–2.4 keV absorption-corrected PSPC count rate to which our survey is complete. Using PIMMS, we have converted this count rate to a 0.2–2.4 keV unabsorbed PSPC flux, 1×10^{-13} ergs cm^{-2} s^{-1} . The above conversion was

performed using the median spectral index ($\Gamma = 4.0$) of the large-amplitude X-ray outbursts in our survey. Because we have defined large-amplitude X-ray outbursts to be sources whose luminosity drops by a minimum factor of 20 between the RASS and pointed PSPC observations, the characteristic absorption-corrected RASS flux to which we are complete is equal to 20 times the characteristic absorption-corrected PSPC flux, or 2×10^{-12} ergs cm^{-2} s^{-1} .

The median 0.2–2.4 keV outburst (RASS) luminosity of the outbursts detected in our survey is $L_{\text{outburst}} = 2.8 \times 10^{43}$ ergs s^{-1} . The characteristic distance to which we are complete is therefore ≈ 342 Mpc, corresponding to $z \approx 0.091$. Our survey has consequently covered a volume of $V_{\text{survey}} \approx 1.68 \times 10^8$ Mpc^3 . Because large-amplitude X-ray outbursts decay over a period of months to years, the majority of outbursts that flared from the 6 months preceding the RASS to the end of the 6 month RASS and for which pointed PSPC observations exist should have been found by our survey. We therefore consider our observed rates to be those for a period of approximately 1 yr. To determine the effect of the X-ray “*K*-correction” on our completeness, we simulated redshifted spectra with the median properties listed above using XSPEC (Arnaud 1996). The *K*-correction causes the observed count rate to drop by $\approx 27\%$ at our completeness limit of $z = 0.091$; we consequently neglect this effect because it is significantly smaller than the geometric dilution factor.

4. DISCUSSION AND CONCLUSIONS

4.1. Constraints

To place constraints on the rate of large-amplitude X-ray outbursts in the local universe, we consider first the case in which all outbursts from galaxies and AGNs have been included in the $\log N$ – $\log S$ fit and for which the power-law index is fixed at $\alpha = -3/2$. Although it is possible that the outbursts from active and inactive galaxies arise from different mechanisms, these events are still poorly understood, making such a calculation worthwhile. The outburst rates derived from all fits can be found in Table 3. For the fit described above, ≈ 42 outbursts should have occurred throughout the entire sky down to our characteristic completeness flux of 2×10^{-12} ergs cm^{-2} s^{-1} . We assume a space density, 1.4×10^{-2} Mpc^{-3} , that is the sum of the inactive galaxy space density and the active galaxy space density. The inactive galaxy space density of 1.35×10^{-2} Mpc^{-3} is the sum of a spiral galaxy space density of 1×10^{-2} Mpc^{-3} (e.g., de Jong 1996) and an E+S0 space density of 3.5×10^{-3} Mpc^{-3} (e.g., Magorrian & Tremaine 1999). We assume an active galaxy space density of 5×10^{-4} Mpc^{-3} (e.g., Peterson 1997). The outburst rate for all galaxies and AGNs is then 1.8×10^{-5} galaxy $^{-1}$ yr $^{-1}$. If intrinsic absorption is important, this rate will be higher; this effect is discussed in detail below for the case in which only outbursts from inactive galaxies are included in the $\log N$ – $\log S$ fit.

When only the outbursts from inactive galaxies are considered, we calculate an outburst rate of 9.1×10^{-6} galaxy $^{-1}$ yr $^{-1}$. This rate corresponds to a timescale of 1.1×10^5 yr between outbursts for a given inactive galaxy. Because this rate lies within the predicted maximum rates for tidal disruption events in inactive galaxies (see § 1), this result pro-

vides additional support for the hypothesis that large-amplitude X-ray outbursts from inactive galaxies are the result of stellar tidal disruptions by SMBHs. In addition, this rate implies that down to 0.02 counts s^{-1} , the typical count rate of a source is the RASS Faint Source Catalog (RASS-FSC),⁹ ≈ 2000 outbursts from inactive galaxies should have occurred during the RASS. This result is in agreement with the prediction of Sembay & West (1993; see § 1). We note that if intrinsic absorption prevents large-amplitude X-ray outbursts from being discovered, this rate will increase. This effect was investigated in § 5 of Sembay & West (1993); they estimate that X-ray outbursts could be detected from only approximately one-half of all spiral galaxies. If we assume, from the respective number densities of spiral and E+S0 galaxies, that $\approx 40\%$ of the inactive galaxies sampled by our survey are such roughly edge-on spirals, an outburst would be detectable from only $f \approx 60\%$ of the galaxies in our sample. Consequently, the outburst rate would rise to 1.5×10^{-5} galaxy $^{-1}$ yr $^{-1}$. Given the uncertainty on f , however, we perform all calculations under the assumption that f is equal to unity.

If we consider only the two active galaxies in our sample for the case in which $\alpha = -3/2$, we obtain an active galaxy outburst rate of 8.5×10^{-4} galaxy $^{-1}$ yr $^{-1}$. This rate is substantially higher than that for inactive galaxies. Because of the theoretical uncertainties associated with the tidal disruption of a star in an active galaxy, predictions of the rate of such events have not yet been made. Consequently, it is difficult to determine whether the derived outburst rate for active galaxies is consistent with the stellar tidal disruption scenario. The dynamics of a stellar tidal disruption event are expected to differ for a galaxy in which an accretion disk is present. It is thought that interactions between a star and the accretion disk of an active galaxy may allow the star to lose momentum and energy and reach a radius at which tidal disruption could occur (e.g., Syer, Clarke, & Rees 1991; Armitage, Zurek, & Davies 1996); the effect that this interaction would have on the rate of disruption is not yet clear. The high apparent rate of outbursts from AGNs, however, suggests that at least some of these outbursts may be due to another mechanism, such as accretion disk instabilities (e.g., Siemiginowska et al. 1996; Burderi et al. 1998), which could lead to variations in the soft excess.

4.2. Predictions for Future Work

In order to place tighter constraints on the outburst rates of both active and inactive galaxies, additional outbursts need to be detected. It would also be useful if the outbursts could be followed up in order to (1) determine their decay rates, (2) measure their X-ray spectra, and (3) look for associated spectroscopic signatures in other bands. In the future, cross-correlations of *ROSAT*, *XMM-Newton*, and *Chandra* data may provide a means by which to identify further outbursts. Assuming that *XMM-Newton* operates for ≈ 10 yr at 70% efficiency, taking observations with a mean length of 40 ks, it will produce ≈ 5500 observations. If ≈ 1000 of these observations overlap and $\approx 30\%$ are in the Galactic plane, *XMM-Newton* should produce ≈ 3200 distinct extragalactic observations. Of these observations, $\approx 35\%$ should have column densities $\geq 3.8 \times 10^{20}$ cm^{-2} , the highest column density

⁹ See <http://www.xray.mpe.mpg.de/rosat/survey/rass-fsc/>.

through which an outburst in our survey was detected. Consequently, ≈ 2100 observations will be useful for identifying large-amplitude X-ray outbursts. The EPIC PN camera, which is the *XMM-Newton* instrument most sensitive to soft X-rays, has a field of view of ≈ 718 arcmin². Approximately one-half of this area, ≈ 359 arcmin², is of sufficient sensitivity to detect these outbursting objects in quiescence for a 40 ks exposure. Consequently, *XMM-Newton* will cover $\approx 0.5\%$ of the extragalactic, low Galactic column density sky. Cross-correlation of these data with the RASS catalogs should allow the identification of all RASS outbursts with outburst count rates ≥ 0.02 counts s⁻¹, the typical count rate of a source in the RASS-FSC. A count rate of 0.02 counts s⁻¹ corresponds to an outburst flux of $\approx 9 \times 10^{-14}$ ergs cm⁻² s⁻¹. Consequently, cross-correlation between RASS and *XMM-Newton* observations should result in the detection of ≈ 22 RASS outbursts. We have carried out a similar calculation for *Chandra* and find that, if *Chandra* were highly sensitive in the 0.2–0.3 keV band, it could identify ≈ 13 RASS outbursts. The back-illuminated and front-illuminated ACIS CCD chips, however, are sensitive down to ≈ 0.3 and ≈ 0.5 keV, respectively. Because the flux of a typical large-amplitude X-ray outburst drops by a factor of ≈ 10 when the flux from 0.2–0.3 keV is excluded, it will be significantly more difficult to prove variability by a factor of 20 without sensitivity in this energy range. Consequently, only a handful of RASS outbursts could be expected to be detected through cross-correlations of *ROSAT* and *Chandra* data.

Any correlation between all-sky survey and pointed observations or pointed observations and pointed observations will be limited by the complicated selection effects discussed in this paper and perhaps others as well. As such, all-sky monitors, or a new sensitive all-sky survey, would provide the best means by which to detect and study additional outbursts in a uniform manner. Missions such as *Lobster-ISS* (e.g., Parmar 2001), *MAXI* (e.g., Mihara et al. 2000), *ROSITA*,¹⁰ and *Swift* (e.g., Gehrels 2000), however, probably do not have the combined spatial resolution and sensitivity to soft X-rays needed to identify additional outbursts of this type (see Grupe 2002). As such, a new sensitive soft X-ray all-sky survey or all-sky monitor is needed. Based on our fixed- α log N –log S fit for all outbursts from galaxies and AGNs, we find that down to a count rate of 0.02 counts s⁻¹, the typical count rate of a source in the RASS-FSC, ≈ 4400 large-amplitude X-ray outbursts should have occurred during the RASS. Although the Galactic column density toward $\approx 65\%$ of these sources is higher than the maximum Galactic column through which one of the outbursts in our sample was detected, ≈ 1540 outbursts should have occurred in regions of sky where the Galactic column density is sufficiently small. In order to detect and study these events, a second all-sky survey sensitive in the 0.1–2.4 keV range is needed. Such a survey should be deep enough to detect sources with fluxes of $\approx 5 \times 10^{-15}$ ergs cm⁻² s⁻¹, a factor of 20 below the flux of an outburst with a 0.1–2.4 keV

RASS count rate of 0.02 counts s⁻¹. Cross-correlation of the RASS with a new all-sky survey would remove many of the complicated selection effects considered above and would provide an excellent means to increase greatly the number of known outbursts of this type, allowing tighter constraints to be placed on the rate of these outbursts in the universe. A sensitive soft X-ray all-sky monitor would provide an excellent means to detect newly outbursting objects and study them as their fluxes decline. Observations of possible tidal disruption events and accretion disk instabilities in other wavelength bands will also be of use in understanding these events better.

We thank L. Angelini for providing us with the list of PSPC observations used to construct the WGACAT catalog. We also thank R. Ciardullo, M. Corcoran, D. Merritt, S. Sigurdsson, and S. Snowden for helpful discussions. We thank an anonymous referee for comments. We gratefully acknowledge financial support from NSF CAREER award AST 99-83783 (J. L. D., W. N. B.) and the Penn State President's Fund for Undergraduate Research (J. L. D.). Some of the spectra presented here were obtained with the Hobby-Eberly Telescope (HET), which is a joint project of the University of Texas at Austin, the Pennsylvania State University, Stanford University, Ludwig-Maximilians-Universität München, and Georg-August-Universität Göttingen. The HET is named in honor of its principal benefactors, William P. Hobby and Robert E. Eberly. The Marcario Low-Resolution Spectrograph (LRS) is a joint project of the Hobby-Eberly Telescope partnership and the Instituto de Astronomía de la Universidad Nacional Autónoma de México.

APPENDIX

FLARING X-RAY SOURCES NEAR THE GALACTIC PLANE

Although sources in the Galactic plane and sources that varied between pointed observations are not part of our survey (see § 2.1), we extended our search for interesting variable sources to these samples. We obtained optical spectra for several variable objects, all of which are stars. Optical spectroscopy of candidate flaring X-ray sources near the Galactic plane was carried out with three different telescopes on separate occasions, as described in Table A1. Figure 4 shows images of the four fields observed. In each image, we mark the PSPC error circle, and we identify the objects that we observed spectroscopically. In Figure 5, we show a montage of the spectra of these objects, all of which turned out to be stars. It is noteworthy that in two of the four fields we found late M stars (one a dMe star) within or very near the PSPC error circle, which suggests that these are the flaring objects. In the other two fields, the optical objects within or just around the PSPC error circle turned out to be F or G stars, which we regard as unlikely counterparts of the flaring X-ray sources.

¹⁰ See <http://www.xray.mpe.mpg.de/rosita>.

TABLE A1
LOG OF *ROSAT* AND SPECTROSCOPIC OBSERVATIONS

α (J2000.0)	δ (J2000.0)	Amp _{var} ^a	<i>ROSAT</i> Phase	<i>ROSAT</i> Date	CR ^b	Optical Source	Telescope and Instrument	Observation Date and Time (UT)	Time (s)
00 45 28.7	+42 18 50.0	25	RASS	1990 July 12	0.059 ± 0.021	No. 1	KPNO 2.1 m + Goldcam	2000 Sep 24, 06:32:42	600
04 30 38.3	+15 35 19.3	31	Pointed	1993 Jan 31	≤0.00241	No. 2	KPNO 2.1 m + Goldcam	2000 Sep 24, 06:32:42	600
08 12 28.8	-31 14 52.0	78	Pointed	1992 Dec 12	0.037 ± 0.005	No. 1	HET + LRS	2000 Mar 15, 02:32:32	780
20 38 13.0	-00 53 13.2	56	Pointed	1992 Aug 10	0.0012 ± 0.0008
			RASS	1990 Oct 8	0.250 ± 0.026	No. 1	CTIO 1.5 m + CSPEC	2001 Jan 22, 08:28:32	1200
			Pointed	1992 Nov 20	≤0.0032	No. 2	CTIO 1.5 m + CSPEC	2001 Jan 22, 08:28:32	1200
			Pointed	1991 May 11	0.870 ± 0.022	No. 1	KPNO 2.1 m + Goldcam	2000 Sep 24, 05:40:10	600
			Pointed	1992 Nov 16	0.016 ± 0.001	No. 2	KPNO 2.1 m + Goldcam	2000 Sep 24, 05:57:46	1800

^a Observed amplitude of count-rate variability in the 0.1–2.4 keV band.

^b Count rate in the 0.1–2.4 keV energy band in counts s⁻¹.

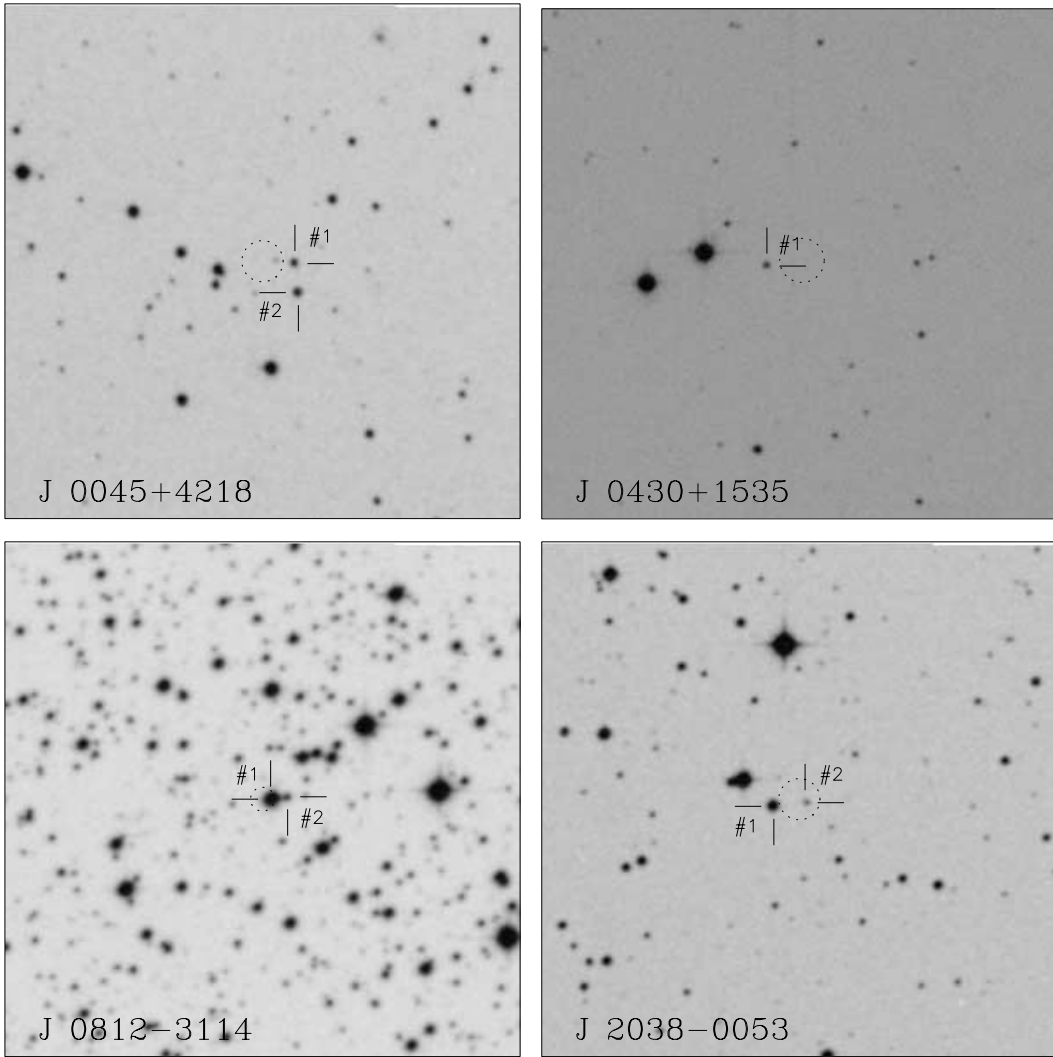


FIG. 4.—Images of the fields of four flaring X-ray sources found near the Galactic plane. These images were drawn from the second generation Palomar Digitized Sky Survey red plates. The size of each field is $5'$, and the coordinates of the center of the field are given in Table A1. The X-ray source error circle is drawn as a dotted circle, and the objects observed spectroscopically are identified. The spectra of these objects are shown in Fig. 5.

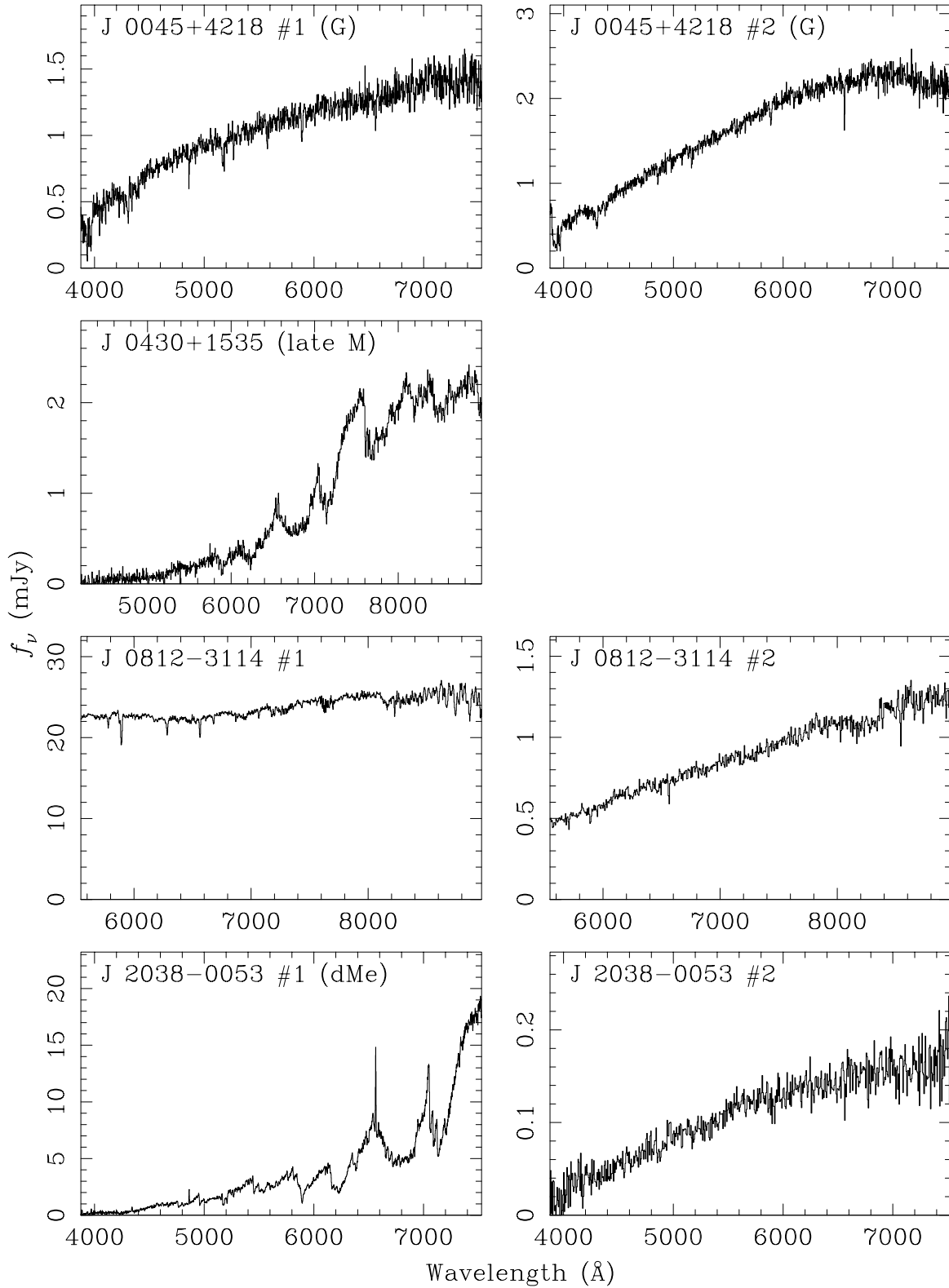


FIG. 5.—Montage of spectra of optical objects in the immediate vicinity of flaring X-ray sources near the Galactic plane. These objects are listed in Table A1 and identified in the images of Fig. 4.

REFERENCES

- Allan, D. J. 1995, ASTERIX User Note 004: Source Searching and Parameterization (Birmingham: Univ. Birmingham)
- Allan, D. J., & Vallance, R. J. 1995, ASTERIX X-Ray Data Processing System (Birmingham: Univ. Birmingham)
- Angelini, L., Park, S., White, N. E., & Giommi, P. 2000, BAAS, 196, 53.10
- Armitage, P. J., Zurek, W. H., & Davies, M. B. 1996, ApJ, 470, 237
- Arnaud, K. A. 1996, in ASP Conf. Ser. 101, Astronomical Data Analysis Software and Systems V, ed. G. Jacoby & J. Barnes (San Francisco: ASP), 17
- Bade, N., et al. 1998, A&AS, 127, 145
- Bade, N., Komossa, S., & Dahlem, M. 1996, A&A, 309, L35
- Boese, F. G. 2000, A&AS, 141, 507
- . 2002, in preparation
- Brandt, W. N., Boller, Th., Fabian, A. C., & Ruszkowski, M. 1999, MNRAS, 303, L53
- Brandt, W. N., Pounds, K. A., & Fink, H. 1995, MNRAS, 273, L47
- Burderi, L., King, A. R., & Szuszkiewicz, E. 1998, ApJ, 509, 85
- Cappellari, M., Renzini, A., Greggio, L., di Serego Alighieri, S., Buson, L. M., Burstein, D., & Francesco, B. 1999, ApJ, 519, 117
- Carrasco, L., Tovmassian, H. M., Stepanian, J. A., Chavushyan, V. H., Erastova, L. K., & Valdés, J. R. 1998, AJ, 115, 1717
- de Jong, R. S. 1996, A&A, 313, 45
- de Vaucouleurs, G. 1991, Observatory, 111, 122
- Eracleous, M., Livio, M., Halpern, J. P., & Storchi-Bergmann, T. 1995, ApJ, 438, 610
- Ferrarese, L., & Merritt, D. 2000, ApJ, 539, L9
- Frank, J., & Rees, M. J. 1976, MNRAS, 176, 633
- Gebhardt, K., et al. 2000, ApJ, 539, L13
- Gehrels, N. 1986, ApJ, 303, 336
- . 2000, Proc. SPIE, 4140, 42
- Greiner, J., Schwarz, R., Zharikov, S., & Orio, M. 2000, A&A, 362, L25
- Grupe, D. 2002, in New Visions of the X-ray Universe in the XMM-Newton and Chandra Era (Noordwijk: ESA), in press
- Grupe, D., Beuermann, K., Mannheim, K., Bade, N., Thomas, H.-C., de Martino, D., & Schwöpe, A. 1995a, A&A, 299, L5
- Grupe, D., Beuermann, K., Mannheim, K., Thomas, H.-C., Fink, H. H., & de Martino, D. 1995b, A&A, 300, L21
- Grupe, D., Thomas, H.-C., & Leighly, K. M. 1999, A&A, 350, L31
- Guainazzi, M., Marshall, W., & Parmar, A. N. 2001, MNRAS, 323, 75
- Gurzadyan, V. G., & Ozernoy, L. M. 1980, A&A, 86, 315
- Heiles, C., & Cleary, M. N. 1979, Australian J. Phys. Astrophys. Suppl., 47, 1
- Ho, L. C., Filippenko, A. V., & Sargent, W. L. W. 1995, ApJS, 98, 477
- Komossa, S., & Bade, N. 1999, A&A, 343, 775
- Komossa, S., & Dahlem, M. 2002, in MAXI Workshop on AGN Variability, ed. N. Kawai, H. Negoro, A. Yoshida, & T. Mihara (Riken: Seiyō), 175
- Komossa, S., & Greiner, J. 1999, A&A, 349, L45
- Li, L. X., Narayan, R., & Menou, K. 2002, ApJ, in press
- Loeb, A., & Ulmer, A. 1997, ApJ, 489, 573
- Magorrian, J., & Tremaine, S. 1999, MNRAS, 309, 447
- Makishima, K., et al. 2000, ApJ, 535, 632
- Merritt, D., & Ferrarese, L. 2001, MNRAS, 320, L30
- Micela, G., Sciortino, S., Kashyap, V., Harnden, F. R., Jr., & Rosner, R. 1996, ApJS, 102, 75
- Mihara, T., et al. 2000, Adv. Space Res., 25(3–4), 897
- Mukai, K. 2000, PIMMS Version 3.0 Users' Guide (Greenbelt: NASA/GSFC)
- Packer, D. 1891, English Mech., 1389, 239
- Parmar, A. N. 2001, Observatory, 121, 1164
- Peterson, B. M. 1997, An Introduction to Active Galactic Nuclei (Cambridge: Cambridge Univ. Press)
- Piro, L., Massaro, E., Perola, G. C., & Molteni, D. 1988, ApJ, 325, L25
- Rees, M. J. 1990, Science, 247, 817
- Renzini, A., Greggio, L., di Serego-Alighieri, S., Cappellari, M., Burstein, D., & Bertola, F. 1995, Nature, 378, 39
- Schlegel, E. M. 1995, Rep. Prog. Phys., 58, 1375
- Sembay, S., & West, R. G. 1993, MNRAS, 262, 141
- Siemiginowska, A., Czerny, B., & Kostyunin, V. 1996, ApJ, 458, 491
- Stark, A. A., Gammie, C. F., Wilson, R. W., Bally, J., Linke, R. A., Heiles, C., & Hurwitz, M. 1992, ApJS, 79, 77
- Storchi-Bergmann, T., Eracleous, M., Ruiz, M. T., Livio, M., Wilson, A. S., & Filippenko, A. V. 1997, ApJ, 489, 87
- Syer, D., & Clarke, C. J. 1992, MNRAS, 255, 92
- Syer, D., Clarke, C. J., & Rees, M. J. 1991, MNRAS, 250, 505
- Veron-Cetty, M. P., & Veron, P. 1998, A Catalogue of Quasars and Active Nuclei (8th ed.; Garching: ESO)
- Voges, W., et al. 1999, A&A, 349, 389